C-CROC: Continuous and Convex Resolution of Centroidal dynamic trajectories for legged robots in multi-contact scenarios

Pierre Fernbach, Steve Tonneau, Olivier Stasse, Justin Carpentier and Michel Taïx

***Abstract*—Synthesizing legged locomotion requires planning one or several steps ahead (literally): when and where, and with which effector should the next contact(s) be created between the robot and the environment? Validating a contact candidate implies *a minima* the resolution of a slow, non-linear optimization problem, to demonstrate that a Center Of Mass (COM) trajectory, compatible with the contact transition constraints, exists.**

We propose a conservative reformulation of this trajectory generation problem as a convex 3D linear program, CROC (Convex Resolution Of Centroidal dynamic trajectories). It results from the observation that if the COM trajectory is a polynomial with only one free variable coefficient, the non-linearity of the problem disappears. This has two consequences. On the positive side, in terms of computation times CROC outperforms the state of the art by at least one order of magnitude, and allows to consider interactive applications (with a planning time roughly equal to the motion time). On the negative side, in our experiments our approach finds a majority of the feasible trajectories found by a non-linear solver, but not all of them. Still, we demonstrate that the solution space covered by CROC is large enough to achieve the automated planning of a large variety of locomotion tasks for different robots, demonstrated in simulation and on the real HRP-2 robot, several of which were rarely seen before.

Another significant contribution is the introduction of a Bezier curve representation of the problem, which guarantees that the constraints of the COM trajectory are verified continuously, and not only at discrete points as traditionally done. This formulation is lossless, and results in more robust trajectories. It is not restricted to CROC, but could rather be integrated with any method from the state of the art.

***Index Terms*—Multi contact locomotion, centroidal dynamics, Humanoid robots, legged robots, motion planning**

I. Introduction

THIS paper is concerned with the issue of planning multi-contact motions for legged robots in human environments.

The term "multi-contact motion" has been proposed to distinguish the problem from the gaited locomotion one [1], [2]. Gaited motions result from the contact interactions created and broken periodically between the end effectors and a flat terrain. The multi-contact problem is more general as it can include non horizontal contacts, and is not restricted to a cyclic strategy. This results in a combinatorial problem in the choice of the contacts being created. It also requires a more complex formulation of the dynamics that govern the motion. This non-linear problem remains open to this date.

Steve Tonneau is at the University of Edinburgh, Scotland.

The other authors are with LAAS-CNRS / Université de Toulouse, France. e-mail: pfernbach@laas.fr

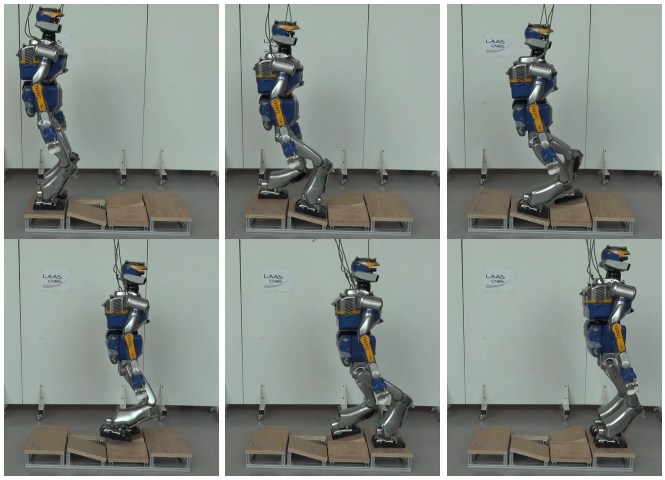

Fig. 1: An instance of the transition feasibility problem: can we guarantee that the contact sequence shown in this picture can be used to produce a feasible motion for the robot? To address this issue in this example we need to account for 9 different contact phases (including phases where the effector is flying, as displayed in the fourth image).

One key issue of multi-contact locomotion consists in choosing contact locations such that the contacts can be broken or created at a given time without violating dynamic or geometric constraints. To tackle this issue one option is to simultaneously optimize the contact locations and the motion of the robot. The problem is non-linear, though promising results have been obtained using approximations [3]–[6]. Such approximations include ignoring collision avoidance or considering a point-mass model.

The present paper lies in the continuity of an alternate approach that decomposes the problem into a sequence of smaller ones [7]–[11].In such approaches, the computation of a contact plan is achieved prior to the motion generation. This simplifies the problem, but introduces the question of the validity (feasibility) of the contact plan.

Those approaches thus face the same fundamental challenge: how to make sure that the solution computed using a reformulation of the multi-contact problem provides a straightforward solution to the original problem? As an example, both families of approaches propose contributions that rely on a model-based approach called the *centroidal model*, which only considers the dynamics of the Center Of Mass of the robot,

rather than the whole-body dynamics. This model introduces approximations regarding the geometric constraints that lie on the robot, and also regarding the angular momentum variation induced by the motion of the rigid bodies that compose the robot. The question is then to determine whether it is possible to formulate additional constraints on the centroidal dynamics, that would take into account the whole-body constraints.

Finding what we call the "reduction properties": formal theorems or empirical properties that will prove the validity of the problem decomposition or approximation, is the original scientific issue that we propose to tackle.

In particular, in this work, we consider what we call the **transition feasibility** problem: given two states of the robot, can we guarantee that there exists (or not) a dynamically and kinematically consistent motion that connects these two states (Figure 1)? Being able to address efficiently this issue is desirable in the context of the authors' framework, but not only, as the objective is to provide additional guarantees to the centroidal model, and to improve significantly its computational efficiency. From an applicative point of view, its resolution would also allow to address the N-step capturability problem [12]–[14]: given the current state of the robot, determine whether it will be able to come to a stop without falling in at most N steps ($N \geq 0$). This issue is very important to guarantee the safety of the robot and its surroundings.

A. The transition feasibility in a divide and conquer context

Over the last few years, we have proposed a methodology to tackle the multi-contact motion problem, which relies on its decomposition into three sub-problems solved sequentially (Figure 2). This approach follows a "divide and conquer" pattern, with the idea that three sub-problems should be addressed in a sequentially independent fashion: $\mathcal{P}_1$, the planning of a trajectory for the root of the robot, $\mathcal{P}_2$ the generation of a discrete contact sequence along the root's trajectory and $\mathcal{P}_3$ the generation of a whole-body motion from this contact sequence. We have proposed several contributions to each sub-problem [15]–[17], and built a prototype that demonstrated its capability to find solutions for various robots and environments, with interactive computation times (a few seconds of computation for several steps of motion).

The decoupling between each sub-problem allows to break the complexity, and comes with a cost that is the introduction of a feasibility problem: each sub-problem must be solved in the feasibility domain of the next sub-problems: ie. there must exist a sequence of contacts (problem $\mathcal{P}_2$) that can follow the root's trajectory found (solution of $\mathcal{P}_1$), and similarly there must exist a feasible whole-body motion (problem $\mathcal{P}_3$) from the computed contact sequence (solution of $\mathcal{P}_2$). The latter problem is an instance of the transition feasibility problem that we address in this paper (The former was considered in [15]).

It is important to observe that in this context, establishing the transition feasibility as fast as possible is crucial: $\mathcal{P}_2$ is a combinatorial problem, which implies that many contact sequences (thousands) must possibly be tried before finding a feasible contact sequence.

Recent contributions have proposed centroidal trajectory generation methods that could theoretically be used to answer the transition feasibility problem [18]–[20]. However, because of the combinatorial aspect of contact planning, the computational time required by these methods is too important to use a trial-and-error approach to verify the feasibility. Caron et al. recently proposed a computationally efficient method [21], but its application range is restricted to single-contact to single-contact transitions.

The work that is the closest to the present paper is the one of Ponton et al. [22]. By integrating the dynamic constraints inside a mixed-integer programming problem [4], they addressed the transition feasibility problem at the contact planning level. However the constraints are only approximated through a convex relaxation (convex approximation is also done in [23]), and mixed-integer approaches remain subject to combinatorial explosion. The main difference between their formulation and the method presented in this paper lies in the fact that the presented method uses conservative dynamics constraints rather than approximated ones, and is also more computationally efficient.

B. Contributions

The main contribution is the formulation of a **transition feasibility** criterion, able to test if there exists a kinematically and dynamically valid motion that connects two states of the robot, called CROC (which stands for Convex Resolution Of Centroidal dynamic trajectories). Thanks to a conservative and convex reformulation of the problem, this is achieved in a fraction of the computational cost required by standard non-linear solvers. This method also produces a feasible CoM trajectory. This trajectory can be used as a valuable initial guess by a non-conservative non-linear solver to converge towards an optimal solution. Noticeably, this formulation is, along with [24], one of the few **able to continuously guarantee that the computed trajectories respect the constraints of the problem**, when other approaches require to discretize the trajectory and check punctually the constraints.

Thanks to this criterion, we can provide strong guarantees that a computed contact sequence will lead to a feasible whole body motion. This also results in a major technical contribution, as we obtain and demonstrate a framework able to automatically and robustly generate complex motions, both in simulation and on the real HRP-2 robot. The framework is an extension of our previous works: [15] [16] for $\mathcal{P}_1$ and $\mathcal{P}_2$, and [17] [18] for $\mathcal{P}_3$.

This paper is organized as following. In section II, we recall the formal definition of the problem. The main contribution of the paper is presented in section III. We then introduce our complete framework in section V. Finally, we present our experimental results in section VI.

C. Situation of the contribution with respect to the authors previous work

The present paper is an extension of an IROS conference paper [25], where we introduce a convex optimization method

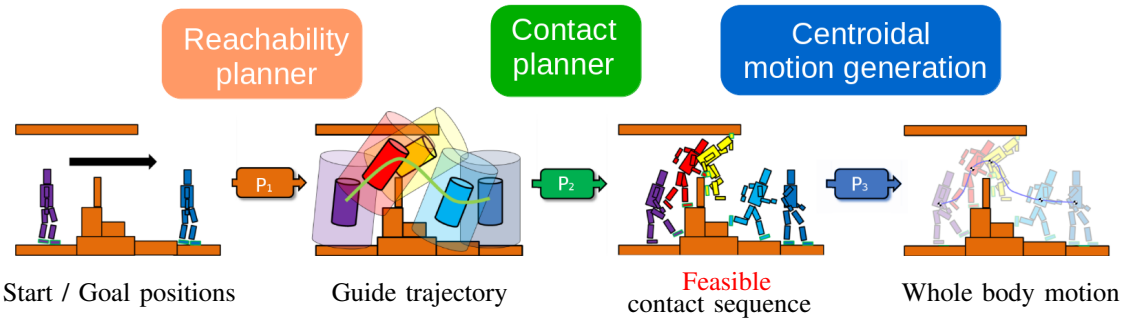

Fig. 2: Complete framework overview of our decoupled approach. In this work we only focus on addressing the transition feasibility problem, from $\mathcal{P}_2$ to $\mathcal{P}_3$.

to solve the transition feasibility problem. Our previous formulation, as others in the community, is limited by the necessity to use of the double description method [26], an unstable mean to compute the linear constraints that apply to the problem [18], which allows for fast computations. As for all existing methods, it also requires a discretization of the solution trajectory, such that the constraints of the problem are only checked at specific instants. This behavior is unsafe as the trajectory between each discretization point is unchecked and may not respect the constraints, as illustrated in Figure 3. In [25], we proposed a continuous formulation of the problem in the simple case of a motion without contact changes, where the trajectory is linearly constrained. In this paper, we extend this continuous formulation to the general setting of a motion with any number of contact transitions. As we will see, this extension is not trivial as it requires handling the non-convex constraint of belonging to a union of polytopes. In addition, this formulation removes the need for discretization of the centroidal trajectory, guaranteeing that the constraints are respected along the whole trajectory. This continuous formulation is also fast enough to avoid using the double description method. The computational gain results from the lower number of variables required to satisfy the constraints.

We advocate for its adoption for any centroidal generation method.

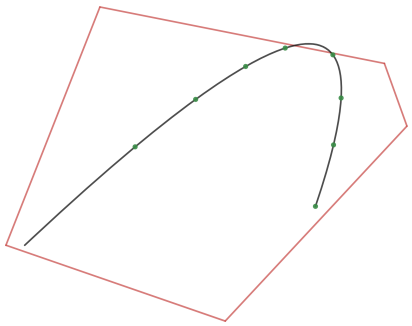

Fig. 3: Example of an invalid solution found by a discretized method. The red lines represent the constraints, wile the black curve is the solution and the green dots are the discretization points. All the discretization points satisfy the constraints while the curve clearly violates them.

Sections II and III present important similarities with respect to [25]. The novelty appears from section III-D, where we present a continuous formulation able to deal with contact switching during the trajectory.

The other sections of the paper are also novel. These novelties include the completion of our experimental framework, which enables us to validate our method on several experiments on the real robot. We also provide an empirical analysis of the performances of our method with respect to a state-of-the-art nonlinear solver, in terms of success rate and computation times.

II. Problem Definition

We define the transition feasibility problem as follows. Given two configurations of a robot; given the contact locations associated to these two configurations; given the position, velocity and acceleration of the Center Of Mass (COM) of the robot at these two configurations; can we guarantee that there exists a **feasible** motion that connects the two configurations? A feasible motion should respect the kinematic constraints of the robot, as well as the dynamics expressed at its CoM. Depending on the use case, some constraints may be removed (for instance if the end configuration is unknown, or if the problem is simply to put the robot to a stop).

Thus, in this work we define the transition feasibility problem with respect to the centroidal dynamics of a robot, as now commonly done in the legged robotics community [27], [19], [18]. In this section we provide some formal definitions that are used in the rest of the paper.

A. Contact sequence and state

A legged motion can be discretized into a sequence of contact phases. Each contact phase defines a number of active contacts, and their locations remain constant during the phase. Thus, each contact phase constrains kinematically and dynamically the motion of the robot. Within a contact sequence, each adjacent contact phase differs by exactly one contact creation or removal (for instance when walking, the contact sequence is gaited and alternates simple and double support phases). The considered contact surfaces are assumed to be rectangular (4 extreme points on each foot) for humanoid robots, and punctual for quadrupedal robots.

We define a state $\mathbf{x} = (\mathbf{c}, \dot{\mathbf{c}}, \ddot{\mathbf{c}}) \in \mathbb{R}^3 \times \mathbb{R}^3 \times \mathbb{R}^3$ as the triplet describing the COM position, velocity and acceleration. To indicate that a state is compatible with the dynamic and kinematic constraints associated with a contact phase $p \in \mathbb{N}$, we use the superscript notation $\mathbf{x}^{\{p\}} = (\mathbf{c}^{\{p\}}, \dot{\mathbf{c}}^{\{p\}}, \ddot{\mathbf{c}}^{\{p\}})$.

Given two states $\mathbf{x}_s^{\{p\}}$ and $\mathbf{x}_g^{\{q\}}$ with $q \geq p$, the transition feasibility problem consists in determining whether there exists a feasible trajectory $\mathbf{c}(t), t \in \mathbb{R}^+$ of duration $T \in \mathbb{R}^+$, which connects exactly $\mathbf{x}_s^{\{p\}}$ and $\mathbf{x}_g^{\{q\}}$.

B. Centroidal dynamic constraints on $\mathbf{c}(t)$

For a contact phase $\{p\}$ of duration T, for any $t \in [0, T]$ the centroidal dynamic constraints are given by the Newton-Euler equations. These constraints form a convex cone (or polytope), which can be expressed under two different formulations, theoretically equivalent [28]–[30], but really different in practice. In this paper we present and discuss both formulations.

1) Equality constraint representation (or force formulation): The Newton-Euler equations are:

$$\begin{bmatrix} m(\ddot{\mathbf{c}} - \mathbf{g}) \\ m\mathbf{c} \times (\ddot{\mathbf{c}} - \mathbf{g}) + \dot{\mathbf{L}} \end{bmatrix} = \begin{bmatrix} \mathbf{I}_3 & ... & \mathbf{I}_3 \\ \hat{\mathbf{p}}_1 & ... & \hat{\mathbf{p}}_{nc} \end{bmatrix} \mathbf{f} \tag{1}$$

Where :

- m is the total mass of the robot;
- nc is the number of contact points;
- $\mathbf{p}_i \in \mathbb{R}^3, 1 \leq i \leq nc$ is the location of the i-th contact point; [1]
- $\mathbf{f} = \begin{bmatrix}\mathbf{f}_1, \mathbf{f}_2, ..., \mathbf{f}_{nc}\end{bmatrix}^T \in \mathbb{R}^{3nc}$ is the stacked vector of contact forces applied at each contact point;
- $\mathbf{g} = \begin{bmatrix}0 & 0 & -9.81\end{bmatrix}^T$ is the gravity vector;
- $\dot{\mathbf{L}} \in \mathbb{R}^3$ is the time derivative of the angular momentum (expressed at $\mathbf{c}$).
- $\hat{\mathbf{p}}_i$ denotes the skew-symmetric matrix of $\mathbf{p}_i$.

The contact forces are further constrained to lie in their so-called friction cone, which we conservatively linearize with four generating rays. Thus $\mathbf{f}$ has the form $\mathbf{f} = \mathbf{V}\boldsymbol{\beta}$, where $\mathbf{V} \in \mathbb{R}^{3nc \times 4nc}$ is the matrix containing the diagonally stacked generating rays of the friction cone of each contact point and $\boldsymbol{\beta} \in \mathbb{R}^{4nc+}$ is a variable.

This formulation has the disadvantage of introducing a large number of variables associated to the contact forces (one vector $\boldsymbol{\beta}$ for each instant where the constraints are verified).

2) Inequality constraint representation (or Double Description formulation): Because the set of admissible contact forces is a polytope, it is possible to use an equivalent "face representation" of the constraints that applies both to the center of mass and the angular momentum quantities. With this formulation, the force variables disappear:

$$\mathbf{H} \underbrace{\begin{bmatrix} m(\ddot{\mathbf{c}} - \mathbf{g}) \\ m\mathbf{c} \times (\ddot{\mathbf{c}} - \mathbf{g}) + \dot{\mathbf{L}} \end{bmatrix}}_{\mathbf{w}} \leq \mathbf{h} \tag{2}$$

where $\mathbf{H}$ and $\mathbf{h}$ are respectively a matrix and a vector defined by the position of the contact points, their normal and their friction coefficients. As this matrix and vector are uniquely defined for a contact phase, we note them with the superscript $\{p\}$ for a contact phase p.

With this formulation, the dimension of the problem is greatly reduced. However, the computation of the matrices $\mathbf{H}^{\{p\}}$ and $\mathbf{h}^{\{p\}}$ is a non-trivial operation called the double description method [26]. It is computationally expensive, and subject to occasional failures.

In the following theoretical sections, we will use the inequality formulation because we believe our contribution is more intuitive with this representation. In terms of implementation the equality formulation is more reliable but slower. However we show that under our formulation the computation times remain in the same order of magnitude with both formulations.

3) The dynamic constraints are not convex: Because of the cross product between $\mathbf{c}$ and $\ddot{\mathbf{c}}$ in the equations (1) and (2), the constraints are bi-linear, leading to a non-convex problem to solve.

C. Centroidal kinematic constraints on $\mathbf{c}(t)$

Each active contact also introduces a kinematic constraint on $\mathbf{c}(t)$, depending of the placement of the end-effectors of the robot. We use a linear constraint formulation to represent this constraint depending on the 6D positions of each active contact frames. They give us a necessary but not sufficient condition for the kinematic feasibility (evaluated and discussed in section IV-G). We refer the reader to [31] for the computation of these constraints. For a given contact phase $\{p\}$ this constraint can be expressed as :

$$\mathbf{K}^{\{p\}}\mathbf{c} \leq \mathbf{k}^{\{p\}} \tag{3}$$

III. Convex formulation of the transition problem

As previously proposed [25], in order to determine the existence of a valid centroidal trajectory $\mathbf{c}(t)$, we formulate the problem as a convex one by getting rid of the non-linear constraints induced by the cross product operation $\mathbf{c} \times \ddot{\mathbf{c}}$. To achieve this we impose a conservative condition on $\mathbf{c}(t)$.

However, a significant contribution with respect to [25] and other contributions is a continuous reformulation of the problem, which guarantees that the resulting trajectory is always valid. Indeed, traditionally the constraints are only verified at specific points of the trajectory, using a discretization step that must be carefully calibrated to avoid an explosion in the number of variables and constraints, while guaranteeing that the constraints will not be violated in between. Figure 3 illustrates the violation of the constraints.

A. Reformulation of $\mathbf{c}(t)$ as a Bezier curve

Let us assume that $\mathbf{c}(t)$ is described by an arbitrary polynomial of degree n of unknown duration T. In such case, without loss of generality, $\mathbf{c}(t)$ is equivalently defined as a constrained Bezier curve of the same degree n:

$$\mathbf{c}(t) = \sum_{i=0}^{n} B_i^n(t/T)\mathbf{P}_i \tag{4}$$

[1] As commonly done, in the case of rectangular contacts (like most robot's feet) we define a contact point at each vertex of the rectangle.

where the B_i^n are the Bernstein polynomials and the $\mathbf{P}_i$ are the control points.

With this formulation we can easily constrain the initial or final positions, velocity or any other derivatives by setting the value of the control points. To exactly connect two states $\mathbf{x}_s = (\mathbf{c}_s, \dot{\mathbf{c}}_s, \ddot{\mathbf{c}}_s)$ and $\mathbf{x}_g = (\mathbf{c}_g, \dot{\mathbf{c}}_g, \ddot{\mathbf{c}}_g)$, we thus need at least 6 control points to ensure that the following constraints are verified:

- $\mathbf{P}_0 = \mathbf{c}_s$ and $\mathbf{P}_n = \mathbf{c}_g$ guarantee that the trajectory starts and ends at the desired locations;
- $\mathbf{P}_1 = \frac{\dot{\mathbf{c}}_s T}{n} + \mathbf{P}_0$ and $\mathbf{P}_{n-1} = \mathbf{P}_n - \frac{\dot{\mathbf{c}}_g T}{n}$ guarantee that the trajectory initial and final velocities are respected;
- $\mathbf{P}_2 = \frac{\ddot{\mathbf{c}}_s T^2}{n(n-1)} + 2\mathbf{P}_1 - \mathbf{P}_0$ and $\mathbf{P}_{n-2} = \frac{\ddot{\mathbf{c}}_g T^2}{n(n-1)} + 2\mathbf{P}_{n-1} - \mathbf{P}_n$ guarantee that the initial and final accelerations are respected.

Depending on the considered problem, some constraints on the boundary positions, velocities or accelerations can be removed, without changing the validity of our approach. For instance, if the objective is simply to put the robot to a stop, the end velocities and accelerations can be set to zero, while the end position is left unconstrained. We can also extend this to any degree and add constraints on initial or final jerk or higher derivatives and automatically compute the position of the control points with a symbolic calculus script such as the one that we provide at the url [2]. We only need to compute the equation of the control points once and for all so we do not need to compute them at runtime. In the following equations, we use a curve of degree 6 with the constraints on initial and final position, velocity and acceleration as described above, and the same reasoning applies to all cases.

B. Conservative reformulation of the transition problem

We now constrain $\mathbf{c}(t)$ to be a Bezier curve of degree $n = 6$. This is a conservative approximation of the transition problem as it does not cover the whole solution space.

As we already need 6 control points to ensure that we connect exactly the two states, this leaves a free control point $\mathbf{P}_3 = \mathbf{y}$:

$$\mathbf{c}(t, \mathbf{y}) = \sum_{i \in \{0,1,2,4,5,6\}} B_i^6(t/T)\mathbf{P}_i + B_3^6(t/T)\mathbf{y} \tag{5}$$

In this case, $\mathbf{y}$ and T are the only variables of the problem. For the time being, we fix T to a constant value. We derive twice to obtain $\ddot{\mathbf{c}}(t)$, and compute the cross product to get the expression of $\mathbf{w}(t)$:

$$\mathbf{w}(t) = \begin{bmatrix} m(\ddot{\mathbf{c}} - \mathbf{g}) \\ m\mathbf{c} \times (\ddot{\mathbf{c}} - \mathbf{g}) + \dot{\mathbf{L}} \end{bmatrix} \tag{6}$$

The non-convexity of the problem disappears, because the cross product of $\mathbf{y}$ by itself is $\mathbf{0}$, and all other terms are either constant or linear in $\mathbf{y}$. $\mathbf{w}(t, \mathbf{y})$ is thus a six-dimensional Bezier curve of degree $2n - 3$ [32] (9 in this case) linearly dependent of $\mathbf{y}$:

[2] http://stevetonneau.fr/files/publications/iros18/derivate.py

$$\mathbf{w}(t, \mathbf{y}) = \sum_{i \in \{0..9\}} B_i^9(t/T)\mathbf{P}_{\mathbf{w}i}(\mathbf{y}) + \dot{\mathbf{L}}(t) \tag{7}$$

where $\mathbf{P}_{\mathbf{w}i}(\mathbf{y}) \in \mathbb{R}^6$ are the control points of $\mathbf{w}(t, \mathbf{y})$ expressed as :

$$\mathbf{P}_{\mathbf{w}i}(\mathbf{y}) = \mathbf{P}_{\mathbf{w}i}^y \mathbf{y} + \mathbf{P}_{\mathbf{w}i}^s \tag{8}$$

The $\mathbf{P}_{\mathbf{w}i}^y \in \mathbb{R}^{6\times 3}$ and $\mathbf{P}_{\mathbf{w}i}^s \in \mathbb{R}^6$ are constants that only depend on the control points $\mathbf{P}_i$ of $\mathbf{c}(t, \mathbf{y})$ and of T.

In what follows, for the sake of simplicity, we assume $\dot{\mathbf{L}}(t) = \mathbf{0}$. This is not a limitation: if we express $\dot{\mathbf{L}}(t)$ as a polynomial in the problem the following reasoning stands. One way to include $\dot{\mathbf{L}}(t)$ is to represent it as a Bezier curve with one or more free variables. However guaranteeing that we can generate a whole-body motion that tracks a variable $\dot{\mathbf{L}}(t)$ requires additional information on the whole-body motion, which we leave as future work [19], [33], [34].

The existence of a valid trajectory $\mathbf{c}(t)$ can thus be determined by solving a convex problem.

C. Application for a motion with no contact switch

We first consider the case where $p = q = 1$.

1) Discrete formulation: Using a discretization step Δt, we discretize $\mathbf{c}(t, \mathbf{y})$ and $\mathbf{w}(t, \mathbf{y})$ over T as follows:

$$\begin{aligned} \mathbf{c}(j\Delta t, \mathbf{y}) &= \quad \mathbf{c}_j^y \mathbf{y} + \mathbf{c}_j^s \\ \mathbf{w}(j\Delta t, \mathbf{y}) &= \quad \mathbf{w}_j^y \mathbf{y} + \mathbf{w}_j^s \end{aligned} \tag{9}$$

Where $\mathbf{c}_j^y$, $\mathbf{c}_j^s$, $\mathbf{w}_j^y$ and $\mathbf{w}_j^s$ are constants given by $\mathbf{P}_{\{0,1,2,4,5,6\}}$, the total duration T and the time step $j\Delta t$. j belongs to the phase set $J^{\{p\}} : \{j \in \mathbb{N} : 0 \leq j\Delta t \leq T^{\{p\}}\}$. Given these expressions, we can replace $\mathbf{w}(t)$ in (2) by its value at each discretization point $j\Delta t$:

$$\mathbf{H}^{\{p\}} \mathbf{w}_j^y \mathbf{y} \leq \mathbf{h}^{\{p\}} - \mathbf{H}^{\{p\}} \mathbf{w}_j^s \tag{10}$$

By proceeding similarly for the kinematic constraint (3), we can formulate the following linear feasibility problem (FP) in 3 dimensions:

$$\begin{aligned} &\textbf{find} \quad \mathbf{y} \\ &\textbf{s.t.} \quad \underbrace{\begin{bmatrix} \mathbf{K}^{\{p\}} \mathbf{c}_j^y \\ \mathbf{H}^{\{p\}} \mathbf{w}_j^y \end{bmatrix}}_{\mathbf{E}_j^{\{p\}}} \mathbf{y} \leq \underbrace{\begin{bmatrix} \mathbf{k}^{\{p\}} - \mathbf{K}^{\{p\}} \mathbf{c}_j^s \\ \mathbf{h}^{\{p\}} - \mathbf{H}^{\{p\}} \mathbf{w}_j^s \end{bmatrix}}_{\mathbf{e}_j^{\{p\}}} \quad \forall j \in J^{\{p\}} \end{aligned} \tag{11}$$

With this discrete formulation the number of constraints in the problem is proportional to the number of discretization points. Moreover, the constraints are verified only at the discretization points, which leaves a risk that a part of the solution trajectory between two discretization points does not satisfy the constraints of the problem (Figure 3). Choosing the number of discretization steps is thus a compromise between the computation time (which depends on the number of constraints) and the risk of finding a solution partially invalid. This is a well-known issue when relying on discretization methods.

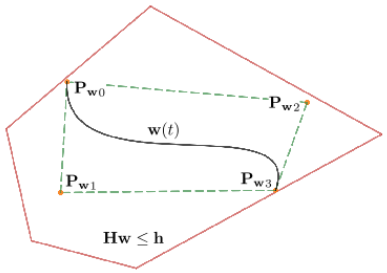

Fig. 4: A bezier curve is comprised in the convex hull of its control points. In this abstract view, the red polygon represents the 6D constraints on $\mathbf{w}(t)$. If the control points $\mathbf{P}_{\mathbf{w}i}$ of $\mathbf{w}(t)$ satisfy the constraints, then the complete curve satisfies the constraints.

2) Continuous formulation: Alternatively, in [25] we proposed a continuous formulation of this problem, only valid for the case where no contact transition occurs. We recall this formulation below as it is fundamental for the following section.

Using the fact that a Bezier curve is comprised in the convex hull of its control points, the main idea of this formulation is to express the kinematic constraints (3) on the control points $\mathbf{P}_i$ of $\mathbf{c}(t, \mathbf{y})$ and the dynamic constraints (2) on the control points $\mathbf{P}_{\mathbf{w}i}(\mathbf{y})$ of $\mathbf{w}(t, \mathbf{y})$ (see Figure 4). Constraining the control points of $\mathbf{w}(t, \mathbf{y})$ to satisfy the constraints of the trajectory is *a priori* a conservative approach that further constrains the solution space (we will see that this limitation can be easily overcome). However, this approach allows for a continuous solution to the problem and guarantees that the trajectory is entirely valid.

Assuming that the start and goal states are feasible (otherwise the problem has no solution), for the kinematic constraints we only need to find a $\mathbf{y}$ that satisfies the constraints. For the dynamic constraints all the control points $\mathbf{P}_{\mathbf{w}i}(\mathbf{y})$ must satisfy the equation (2), given the expression (8) we can express the dynamic constraints as follow:

$$\mathbf{H}^{\{p\}}\mathbf{P}^{y}_{\mathbf{w}i}\mathbf{y} \leq \mathbf{h}^{\{p\}} - \mathbf{H}^{\{p\}}\mathbf{P}^{s}_{\mathbf{w}i}, \forall i \in [0, 2n-3] \tag{12}$$

Finally, we can reformulate the discretized Linear Feasibility Problem (11) in a continuous fashion:

$$\begin{aligned} \textbf{find} \quad & \mathbf{y} \\ \textbf{s.t.} \quad & \mathbf{K}^{\{p\}}\mathbf{y} \leq \mathbf{k}^{\{p\}} \\ & \mathbf{H}^{\{p\}}\mathbf{P}^{y}_{\mathbf{w}i}\mathbf{y} \leq \mathbf{h}^{\{p\}} - \mathbf{H}^{\{p\}}\mathbf{P}^{s}_{\mathbf{w}i} \quad , \forall i \end{aligned} \tag{13}$$

In this case, the whole trajectory necessarily satisfies the constraints everywhere, as they form a convex set.

D. Application to a motion with one contact switch

We now consider the case where $q = p+1$. In this case we define $T^{\{p\}}$ and $T^{\{q\}}$ as the time spent in each phase, such that $T = T^{\{p\}} + T^{\{q\}}$.

When a contact switch occurs during a motion, the constraints applied to the COM trajectory change at the switching time $t = T^{\{p\}}$. When $t < T^{\{p\}}$, the constraints of phase $\{p\}$ must be applied and conversely, the constraints of phase $\{q\}$ must be applied and when $t > T^{\{p\}}$. At $t = T^{\{p\}}$, the constraints of both phases must be applied.

1) Discrete formulation: Adapting the discretized FP (11) to this case is straightforward: the formulation remains the same, with the only difference that the constraints that must be verified at each discretized point change at $t = T^{\{p\}}$ and $t > T^{\{p\}}$. We thus have 3 sets of constraints in this case: one for each of the two phases, plus one for the transition time $t = T^{\{p\}}$ where the constraints of both phases apply. We define $J^{\{q\}} : \{j \in \mathbb{N}, T^{\{q-1\}} \leq j\Delta t \leq T^{\{q\}}\}$ and obtain the following FP:

$$\begin{aligned} \textbf{find} \quad & \mathbf{y} \\ \textbf{s.t.} \quad & \mathbf{E}^{\{z\}}_{j}\mathbf{y} \leq \mathbf{e}^{\{z\}}_{j} \quad , \forall j \in J^{\{z\}}, \forall z \in \{p, q\} \end{aligned} \tag{14}$$

2) Continuous formulation: In this case, since $\mathbf{w}(t)$ spans 2 distinct sets of linear inequalities, the convex hull of its control points is not guaranteed to lie in the constraint set. The key idea, unlike Lengagne et al. [24], is to fall back to the case where no contact switch occurs, by considering two curves that continuously connect at the switching time $T^{\{p\}}$. A similar approach has been proposed before, in the context of UAVs [35], with the difference that in our case the continuity of the trajectory is guaranteed by the De Casteljau decomposition algorithm. This algorithm divides the original curve into two curves $\mathbf{c}(t, \mathbf{y})$, each curve being subject to the constraints of their respective contact phase (see Figure 5). The result is thus the expression of the control points of two Bezier curves $\mathbf{c}_{\{p\}}(t, \mathbf{y})$ and $\mathbf{c}_{\{q\}}(t, \mathbf{y})$ with the same degree as the original curve, such that :

$$\begin{cases} \mathbf{c}_{\{p\}}(t, \mathbf{y}) = \mathbf{c}(t, \mathbf{y}) & \forall t \in [0; T^{\{p\}}] \\ \mathbf{c}_{\{q\}}(t, \mathbf{y}) = \mathbf{c}(t, \mathbf{y}) & \forall t \in [T^{\{p\}}; T] \end{cases} \tag{15}$$

The De Casteljau decomposition guarantees that $\mathbf{c}_{\{p\}}(T^{\{p\}}, \mathbf{y}) = \mathbf{c}_{\{q\}}(T^{\{p\}}, \mathbf{y})$, and that the composition of the curves in infinitely differentiable ($\mathcal{C}^{\infty}$), as it is strictly equivalent to $\mathbf{c}(t, \mathbf{y})$. The control points of the new curves are linearly dependent on the control points of the original un-split curve, and thus have the following form:

$$\mathbf{c}_{\{z\}}(t, \mathbf{y}) = \sum_{i=0}^{n} B_i^n(t/T^{\{z\}})\mathbf{P}_i^{\{z\}}(\mathbf{y}) \quad \forall z \in \{p, q\} \tag{16}$$

where the $\mathbf{P}_i^{\{z\}}(\mathbf{y})$ have the form:

$$\mathbf{P}_i^{\{z\}}(\mathbf{y}) = \mathbf{P}_i^{y\{z\}}\mathbf{y} + \mathbf{P}_i^{s\{z\}} \tag{17}$$

with $\mathbf{P}_i^{y\{z\}}$ and $\mathbf{P}_i^{s\{z\}}$ constants.

It follows that $\mathbf{w}_{\{p\}}(t, \mathbf{y})$ and $\mathbf{w}_{\{q\}}(t, \mathbf{y})$ are also linearly dependent of $\mathbf{y}$:

$$\begin{aligned} \mathbf{w}_{\{z\}}(t, \mathbf{y}) &= \sum_{j=0}^{2n-3} B_j^{2n-3}(t/T^{\{z\}})\mathbf{P}_{\mathbf{w}j}^{\{z\}}(\mathbf{y}) \\ \text{with } \mathbf{P}_{\mathbf{w}j}^{\{z\}}(\mathbf{y}) &= \mathbf{P}_{\mathbf{w}j}^{y\{z\}}\mathbf{y} + \mathbf{P}_{\mathbf{w}j}^{s\{z\}} \quad , \forall z \in \{p, q\} \end{aligned} \tag{18}$$

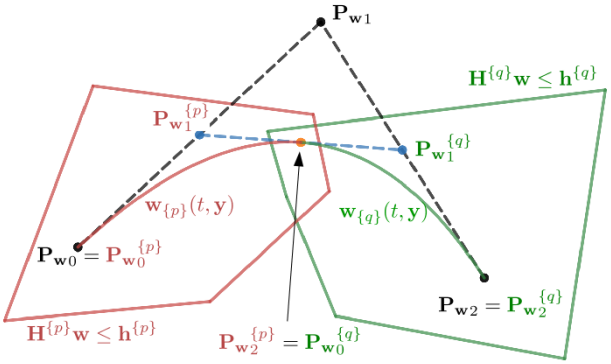

Fig. 5: Example of curve decomposition with the De Casteljau algorithm. The original curve comprises 3 control points (black). It is decomposed into two curves comprising the same number of control points each (3). We can then constrain the control points of the first curve (red) to lie in the first set of constraints, and similarly constrain the control points of the second curve (green) to lie in the second set of constraints. As a result, if the constraints can be satisfied, the connecting control point of both curves satisfies both set of constraints, and we obtain the guarantee that each sub-curve satisfies its respective set of constraints. Interestingly, the control points of the sub-curves are constrained to belong to their respective cones, but those of the original curve can lie outside of the constraints.

Finally the constraints of (13) can be rewritten to deal with the contact switches. The kinematic constraints expressed at each control points are written:

$$\underbrace{\mathbf{K}^{\{z\}}\mathbf{P}_i^{y\{z\}}}_{\mathbf{A}_i^{\{z\}}}\mathbf{y} \leq \underbrace{\mathbf{k}^{\{z\}} + \mathbf{K}^{\{z\}}\mathbf{P}_i^{s\{z\}}}_{\mathbf{a}_i^{\{z\}}}, \forall i, \forall z \in \{p, q\} \quad (19)$$

and the dynamic constraints:

$$\underbrace{(\mathbf{H}^{\{z\}}\mathbf{P}_{\mathbf{w}j}^{y\{z\}}}_{\mathbf{D}_j^{\{z\}}}\mathbf{y} \leq \underbrace{\mathbf{h}^{\{z\}} - \mathbf{H}^{\{z\}}\mathbf{P}_{\mathbf{w}j}^{s\{z\}}}_{\mathbf{d}_j^{\{z\}}}, \quad \forall j, \forall z \in \{p, q\} \quad (20)$$

We can then stack the constraints:

$$\mathbf{A} = \begin{bmatrix} \mathbf{A}_0^{\{p\}} \\ \vdots \\ \mathbf{A}_n^{\{p\}} \\ \mathbf{A}_0^{\{q\}} \\ \vdots \\ \mathbf{A}_n^{\{q\}} \end{bmatrix} \mathbf{a} = \begin{bmatrix} \mathbf{a}_0^{\{p\}} \\ \vdots \\ \mathbf{a}_n^{\{p\}} \\ \mathbf{a}_0^{\{q\}} \\ \vdots \\ \mathbf{a}_n^{\{q\}} \end{bmatrix} \mathbf{D} = \begin{bmatrix} \mathbf{D}_0^{\{p\}} \\ \vdots \\ \mathbf{D}_{2n-3}^{\{p\}} \\ \mathbf{D}_0^{\{q\}} \\ \vdots \\ \mathbf{D}_{2n-3}^{\{q\}} \end{bmatrix} \mathbf{d} = \begin{bmatrix} \mathbf{d}_0^{\{p\}} \\ \vdots \\ \mathbf{d}_{2n-3}^{\{p\}} \\ \mathbf{d}_0^{\{q\}} \\ \vdots \\ \mathbf{d}_{2n-3}^{\{q\}} \end{bmatrix} \quad (21)$$

We recall that in our case $n = 6$. Finally, we can rewrite FP (13) with a contact switch as:

$$\begin{aligned} \textbf{find} \quad & \mathbf{y} \\ \textbf{s.t.} \quad & \mathbf{A}\mathbf{y} \leq \mathbf{a} \\ & \mathbf{D}\mathbf{y} \leq \mathbf{d} \end{aligned} \quad (22)$$

This boils down to check if each control point of each split curve satisfies the constraints of the current contact phase.

E. General case

In the general case, the same idea will apply. In the continuous case, we use the De Casteljau algorithm to split $\mathbf{c}(t)$ into as many curves as required, thus falling back to a formulation with no contact switches. In the discrete case, we assign the appropriate constraints for each discretized time step. While these decompositions appear mathematically heavy, from a programming point of view, they can be automatically generated, and thus are in fact simple to implement.

In our experiments, we only consider three consecutive phases (which correspond to one step), and solve a new problem for each subsequent set of phases. We call one such convex problem "*CROC*", which stands for *Convex Resolution Of Centroidal dynamic trajectories*.

F. Non-conservative continuous formulation

The presented continuous formulation is more conservative than the discretized one. Constraining the control points to lie inside the constraint set prevents from the generation of curves such as the one illustrated in Figure 6.

However, by relying on the De Casteljau algorithm, it is possible to continuously satisfy the constraints while considering control points outside of the constraint set. Indeed when a curve is split, the constraints no longer apply to the control points of the original curve, but to the control points of the sub-curves. This is illustrated in Figure 5. If the curve is split an infinite number of times, it is straightforward to see that the original curve can span entirely its original definition set as the position of the control points converge to the original curve as the number of split increase.

The price to pay is that the number of constraints increases with the number of curve splittings: a curve of degree s split b times comprises $(s+1) * (b+1)$ constraints. The higher the number of splits is, more the number of constraints to address increases. A parallel can be made with the discretized approach: the lower the discretization step is, the higher the number of constraints is.

We believe that a deeper analysis of the pros and cons of using a continuous formulation, not only in the case of CROC, but with any other formulation of the problem, requires a significant amount of research, and thus will be discussed in a future work. In this paper, we only divide the curve at the transition points, and we show in our experiments that this is already sufficient to perform similarly to the discretized approaches, while ensuring comparable time performances.

G. Cost function and additional constraints

As the transition feasibility problem is addressed by CROC, a feasible COM trajectory is computed. It is possible to

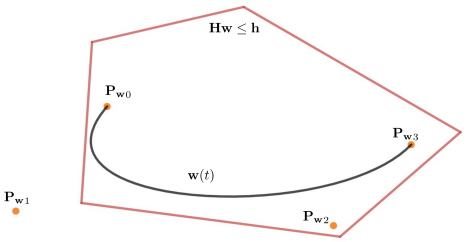

Fig. 6: The curve $\mathbf{w}(t)$ belongs entirely to the convex boundaries (red), while a control point $\mathbf{P_{w1}}$ lies outside of them.

optimize this trajectory to minimize a given cost function $l(\mathbf{y})$, either linear or quadratic. In the latter case the FP problem (22) then becomes a Quadratic Program (QP). One can for instance minimize the integral of the squared acceleration norm or the angular momentum. This cost function is irrelevant to solve the transition feasibility problem, but it can be later used as a reference COM trajectory for a whole-body motion generator, or as an initial guess for a nonlinear solver as discussed in Section IV-F.

The formulation also allows to add inequality constraints on $\mathbf{c}$ and any of its derivatives by rewriting the expression of the control points of the desired curve as done in equation (17). Here again, these constraints can either be verified continuously on the concerned control points, or in a discretized fashion. In any case, they take the form:

$$\mathbf{O}\mathbf{y} \leq \mathbf{o} \tag{23}$$

We use such constraints to impose bounds on the velocity and acceleration of the center of mass or on the angular momentum variation. The most generic form of our continuous problem is thus the following QP:

$$\begin{aligned} \mathbf{find} \quad & \mathbf{y} \\ \mathbf{min} \quad & l(\mathbf{y}) \\ \mathbf{s.t.} \quad & \mathbf{A}\mathbf{y} \leq \mathbf{a} \\ & \mathbf{D}\mathbf{y} \leq \mathbf{d} \\ & \mathbf{O}\mathbf{y} \leq \mathbf{o} \end{aligned} \tag{24}$$

In our experiments we set constraints on the acceleration and velocity and minimize the squared acceleration norm as a cost l. In the remainder of the paper "*CROC*" refers to this generic QP. If nothing is specified, by default *CROC* refers to the continuous formulation and with the inequalities representation of the dynamic constraints, as in the QP (24).

H. Time sampling

In the previous sections, in order to remain convex when computing $\mathbf{w}(t)$ (equation (6)) we assumed that the duration of each phase $T^{\{p\}}, T^{\{p+1\}}$ and $T^{\{p+2\}}$ was given.

Time can be reintroduced in the problem using a bi-level optimization approach [36]. However, in this work we choose a more pragmatic offline-sampling approach to compute relevant timing candidates, which turns out to be lossless among all of our experiment set.

To achieve this, we consider a large variety of instances of the transition problem. We first consider all the scenarios demonstrated in Section VI (for HRP-2 and HyQ), from which we extract instances of the transition problem. We secondly generate random scenarios (Figure 9). We randomly allocate initial and end velocities for the center of mass along the direction of motion, between 0 and 1.5 $m.s^{-1}$.

For a total of 10 000 instances of the transition problem, we sample various combinations of times, solve the corresponding QPs and check whether a solution is found. In theory, this would mean that we need to sample an infinity of time combinations in order to be complete. However, we pragmatically reduce this number and give up on the completeness while maintaining a high success rate as follows: we sampled a time for each duration phase $T^{\{z\}}$ by choosing a value between 0.1 and 2 seconds for phases without end-effector motion and between 0.5 and 2 seconds for phases with end-effector motion, with increments of 50ms. For a sequence of three phases with one phase with end-effector motion, this gives a total of 43320 possible combinations. We tested CROC with all these combinations on various problems : with HRP-2 or HyQ robots on flat and non-coplanar surfaces, for several thousands of states.

Upon analysis of the results of the convergence of the QPs, we found out that we can use a small list of timings combinations (5 in our case, shown in table I) that covers 100% of the success cases for all the robots and scenarios tested. We thus solve a maximum of 5 QPs for each validation. Figure 7 shows the evolution of the success rate according to the number of timings combinations used. We observe that 3 combinations are enough to reach 99% of success but that two additional combinations are required to reach exactly 100%.

The number 100% may appear large. Intuitively however, it seems to highlight the fact that the accuracy of the transition times are not that important for the considered feasibility problem. Indeed $T^{\{p\}}$ constrains the COM trajectory to lie in the intersection of two contact phase constraints at this precise time. However this intersection is in general of a significant volume. As a result the COM trajectory will belong to the intersection for a large time window, which results in a significant slack in the selection of time.

We recall that here, we are only concerned in finding feasible times. For instance, typical double support times when walking on flat ground are closer to 0.2 seconds than 1 second for $T^{\{p\}}$ in dynamical cases. However 0.2 seconds is not feasible when starting from a null velocity. In both cases the interval between 0.8 and 1.2 seconds is almost always feasible in our experiments, which explains why such timings were selected for $T^{\{p\}}$. As such, table I should **not** be considered as a table giving optimal contact time durations, but rather one maximizing feasibility over our set of problems.

IV. Performances of CROC

A. CROC vs a nonlinear solver

Computing the success rate of our method is a hard task because we do not have any way to determine the "ground truth" feasibility of a transition (ie. there does not exist any

timings (s)			Success rate (%)
$T^{\{p\}}$	$T^{\{p+1\}}$	$T^{\{p+2\}}$	
1	0.8	0.8	91.2
1	0.75	0.9	89.2
0.8	0.8	0.9	88.3
0.7	0.5	0.85	77.7
1.2	0.6	1.1	70.8

TABLE I: Success rate with the five used timings combinations.

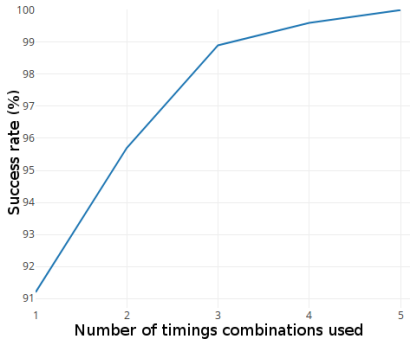

Fig. 7: Evolution of the success rate of CROC according to the number of timings combinations used. Tested on various scenarios with coplanar and non-coplanar contacts and with a bipedal and a quadrupedal robots.

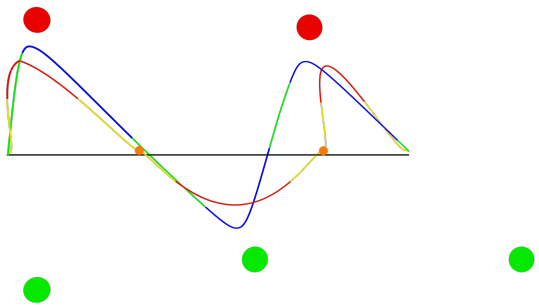

Fig. 8: Example of centroidal trajectories generated with CROC and a nonlinear solver (bird eye view), in a case of bipedal walking. The red and green circles represent the contact positions of the (respectively) left and right feet centers over time. The red and yellow (respectively related to single and double support phases) curve is the curve obtained through the concatenation of curves computed with CROC. The blue and green (respectively related to single and double support phases) curve is obtained through optimization of the latter curve with a nonlinear solver. The orange circles represent the constrained COM positions resulting from the contact planning phase, which are ignored by the nonlinear solver to produce smoother motions.

method able to determine in finite time whether there exists a valid centroidal trajectory between the two states). We choose to compare the relative success rate of CROC with respect to a state-of-the-art non-linear formulation of the same problem [18], which is reported to give similar results to the one from Ponton et al. [22].

Both approaches share similar formulations in terms of kinematic constraints. Conversely the nonlinear solver does not use the conservative formulation of CROC that makes the problem convex, and thus is able to explore a larger part of the solution space, and thus to find a “more optimal” solution of a given locomotion problem.

From a practical point of view, the nonlinear solver is also able to tackle motion synthesis problems over large sequences of contacts. While CROC only interpolates trajectories over two waypoints given by the planner, the non-linear solver is able to ignore the waypoints to find a better solution (Figure 8). This locality is, in our experience, the main source of difference between the trajectories computed by CROC and the nonlinear solver. This difference is what ultimately motivates the use of the nonlinear solver to refine the trajectories obtained by CROC in Section V-C, at a stage where the contact sequence is fixed and the combinatorial is not a problem anymore.

B. Comparison benchmarks

The scenarios used in our benchmarks consist of randomly generated sequences of 3 contact phases such that:

- both initial and final contact phases are in static equilibrium
- both initial and final contact phases have the same effectors in contact, between two and four
- there is exactly one contact repositioning between both initial and final contact phases and no other contact variation
- the intermediate contact phase is not required to be in static equilibrium.

These benchmarks thus only consider the case of a ”repositioning” of an end-effector but as explained in section III-E this is our main use case for CROC as it encompasses the only two other possible cases (creating a contact or breaking a contact) and because this is the kind of contact sequences produced by our contact-planner.

For this benchmark we considered two kind of scenarios. In the first case, we only sample contact phases with coplanar contacts. In the second case, we sample truly random contacts, which lead to contact phases with non-coplanar contacts and contact sequences that require complex motions. Some examples of randomly generated scenarios are shown in Figure 9.

All the benchmarks were run on a single core of an Intel Xeon CPU E5-1630 v3 at 3.7Ghz. The QP problems are solved with QuadProg, and the FP problems with GLPK [37].

The first benchmark compares four different methods: both discrete[3] and continuous formulation of CROC presented in this paper (using the inequality representation of the constraints), the nonlinear resolution proposed in [18] and the same nonlinear method but initialized with the solution found by CROC when available. As we compare the relative success rate between the methods, we only consider the scenarios where at least one of the method finds a solution when computing the percentage of success. The results are shown in table II.

[3]with 7 discretization points per contact phases, which corresponds to a time step of approximately 100ms.

(a) Unfeasible (b) Feasible (c) Feasible (d) Feasible

Fig. 9: Examples of random contact transitions used for benchmarking. Top row : initial configuration, bottom row : final configuration. (a) and (b) only have both feet in contact, (c) and (d) have both feet and the left hand in contact. All the displayed configurations are in static equilibrium, but the intermediate configuration with one less contact (not shown) is not constrained to be in static equilibrium. None of the methods found a solution for the transition (a), the other transitions were successfully solved.

Method	**Coplanar** success (%)	**Non-coplanar** success (%)	Total time (ms)
CROC (discrete)	89.7	60.6	3.89
CROC (continuous)	88.4	57.2	3.93
Non-linear	100	94.1	$\simeq$ 150
N-L with init guess	100	100	$\simeq$ 130

TABLE II: Comparison between CROC and a non linear solver for randomly generated contact sequences of three contact phases. The two first methods are the ones presented in this paper, with either the discrete[3] or continuous formulation and using the inequality representation of the dynamic constraints. These methods are compared with the non linear solver presented in [18], either with their naive initial guess (Non-linear) or with the solution found by CROC as an initial guess when available (N-L with init guess). The percentages on the "success" columns only consider the scenario where at least one method found a solution.

C. How conservative is CROC?

Because of its conservative reformulation, CROC does not cover the whole solution space. As expected, our method finds less solutions than the nonlinear solver. In the coplanar case, CROC almost finds 90% of the solutions. In the non-coplanar case, the centroidal trajectory may be required to present several inflexion points and/or to be really close of the constraints, which cannot be represented using a single variable control point for the trajectory. This explains the difference of success rates between the two cases. However, even in such complex cases CROC still finds around 60% of the solutions.

D. Computation time

As claimed in the introduction, CROC is about two order of magnitude faster than the nonlinear solver that we are using for the centroidal motion generation. Thanks to this efficiency, it is realistic to use our method during the contact planning to evaluate hundreds of candidate transitions.

For the inequality representation with the double description method, the computation time allocated to solve the QP of equation (24) is extremely fast with $50\mu s$ on average. The computation time of CROC, which comprises the time required to solve the QP and the time required to compute all the constraints matrices of equation (21) is around $400\mu s$. The total time in table II also includes the time required by the double description method. However, in some cases the same contact phases may be used several times and the double description method only needs to be computed once per contact phase, thus the time required for the double description may be factorized.

1) Comparison with the equality representation: Table III shows the difference in computation time between the inequality and equality formulation, with a varying number of contacts.

Formulation	Metric	Number of contacts		
		2	3	4
Double-Description	DD time (ms)	3.52	14.88	28.16
	Total time (ms)	3.93	16.18	37.41
Force	Total time (ms)	13.01	25.28	49.65

TABLE III: Comparison between the computation times required to generate and solve the FP[4] defined by CROC using either the Double Description (DD) or the Force formulation.

The major difference between the two representations lies in the dimension of the variables and the constraints of the problem, which is greater in the case of the force formulation. As shown in Table III the computation times between the double description and the force formulations remain in the same order of magnitude for 2 to 4 contacts, with an advantage for the double description. However this advantage reduces as the number of contacts increase. Indeed, while the computation time for the force formulation doubles at each additional contact, the time grows cubicly with the Double Description (DD) formulation.

E. Comparing the continuous and discretized formulations

The results of Table II confirm that the continuous formulation presented in section III-C2 is conservative with respect to the discrete formulation. However, these results show only a marginal difference of success rate between the discrete and continuous formulation of CROC $(1 - 4\%)$. This can first be explained by the fact that the De Casteljau decomposition allows for the control point $\mathbf{y}$ to lie outside of the constraints (Figure 5), thus making the method less restrictive. We propose a second explanation, which is only intuitive (thus not a claim): the remaining missing solutions are necessarily those that will result in the curve lying close to the constraint boundaries. The discretized approach will theoretically find them, but

[4]QP and FP give similar times for the DD formulation, while the FP is much more efficient in the Force formulation. This is only an implementation problem, since GLPK exploits the sparsity of the problem while QuadProg does not.

the chances of finding a trajectory partially outside of the constraint sets are much higher in this case (Figure 3).

Moreover, in section III-D2 we proposed to only split the trajectory in one curve for each contact phases but it is possible to split the trajectory in an arbitrary number of curves, as long as each curve is entirely contained in one contact phases, as detailed in section III-F. By increasing the number of split curves, we can further reduce the loss of solutions.

1) Invalid solutions of the discretized methods: Again, the major drawback of a discretized approach is that the portions of the curve in-between two discretization points are never checked and could violate the constraints (Figure 3).

In order to measure this risk four variants of CROC were compared with the same randomly generated contact sequence as before: the discretized version with three different values of number of discretization points per phases and the continuous version presented in this paper. The four variants use the inequality representation of the dynamic constraints. Then, for each centroidal trajectory found as a solution, the dynamic constraints were verified with a really small discretization step. If the constraints were not satisfied for at least one point of the trajectory, we count this solution as "invalid".

Method	Invalid solutions (%)		Computation time (ms)
	Coplanar	**Non-coplanar**	
Discrete (3 pts)	10.6	19.7	0.20
Discrete (7 pts)	6.7	9.3	0.37
Discrete (15 pts)	4.2	6.9	0.75
Continuous	0	0	0.41

TABLE IV: Comparison between the method CROC with the discrete formulation (D), with varying number of discretization points, and the continuous formulation (C) presented in this paper.

Table IV shows that the percentage of invalid solutions found by the discrete methods is non negligible. Obviously, as the number of discretization points increase this percentage decreases. As shown in equation (11) the number of constraints in the discretized LP problem is proportional to the number of discretization points. Thus the number of discretization points used is a complex parameter to tune, as it is a compromise between the computation time and the risk of finding invalid solutions. This issue is common to all methods that rely on discretization. It emphasizes the fact that we need a continuous method, able to check exactly whether the whole trajectory is valid with a fixed number of constraints in the problem.

2) Computational advantage of the continuous formulation: Depending on the discretization, the continuous formulation can be slower or faster to compute. However, to reach less than 5 % of false positive trajectories with the discretized approach, table IV shows that the continuous formulation is actually faster.

F. Using CROC to initialize a non linear solver

Choosing an initial guess for the nonlinear solver of a trajectory generation method is essential but may be challenging for multi-contact motions. The quality of this initial guess has a significant influence on the convergence of the nonlinear solver. For the nonlinear method considered in this section [18] proposed a naive initial guess of the centroidal trajectory based solely on the position of the contact points.

Interestingly, Table II suggests that the solution set spanned by CROC is not strictly included in the one spanned by this nonlinear solver with this naive initial guess. Using the solution of CROC to initialize the nonlinear solver can thus help it to converge and increase its success rate. As shown in Table II, this improvement only appears for the non-coplanar case because the naive initial guess used is always close to a valid solution in the coplanar case. We expect that the importance of the initial guess will grow if the contact sequences do not allow static equilibrium configurations at the contact phases, and will check this hypothesis in the future.

Moreover, by using the solution of CROC to initialize the nonlinear solver we measured a reduction of the number of iterations required to converge of 20% on average, reducing the total computation time (ie. it is faster to use CROC and then the non-linear solver than using the non-linear solver directly).

G. Validity of our kinematic constraints

As explained in the section II-C, our representation of the kinematics constraints is a necessary but not sufficient approximation. In order to evaluate the accuracy of this approximation, for each feasible transition found by CROC between random configurations, we tested explicitly the kinematic feasibility of the centroidal trajectory with an inverse kinematic. This tests showed that 17.5 % of the trajectories found by CROC were not kinematically valid. This shows that our approximation of the kinematic constraints is not sufficient. However, this is not a limitation of CROC, but rather of the formulation of the kinematic constraints, which we hope to improve in the future.

Moreover, by doing the same tests without any kinematic constraints we found a total of 72.3 % of kinematically unfeasible trajectories. This results show the interest of our kinematic constraints approximation to improve the feasibility of the trajectories found by CROC.

V. Experimental framework

Figure 10 shows the complete framework used for our experiments, implemented with the Humanoid Path Planner [38] framework. The inputs are an initial (respectively goal) position and orientation for the root of the robot, as well as a set of bounds on the velocities and acceleration applying to the COM and the end-effector, and a complete representation of the 3D environment. The output is a dynamically consistent and collision free whole-body motion which can be played on a real robot as shown in section VI.

In this paper, we modify the contact generation method by adding CROC as a feasibility criterion, and connect all the pieces of the framework together. These other pieces are used as black boxes and thus only briefly introduced, with a reference to their respective publications.

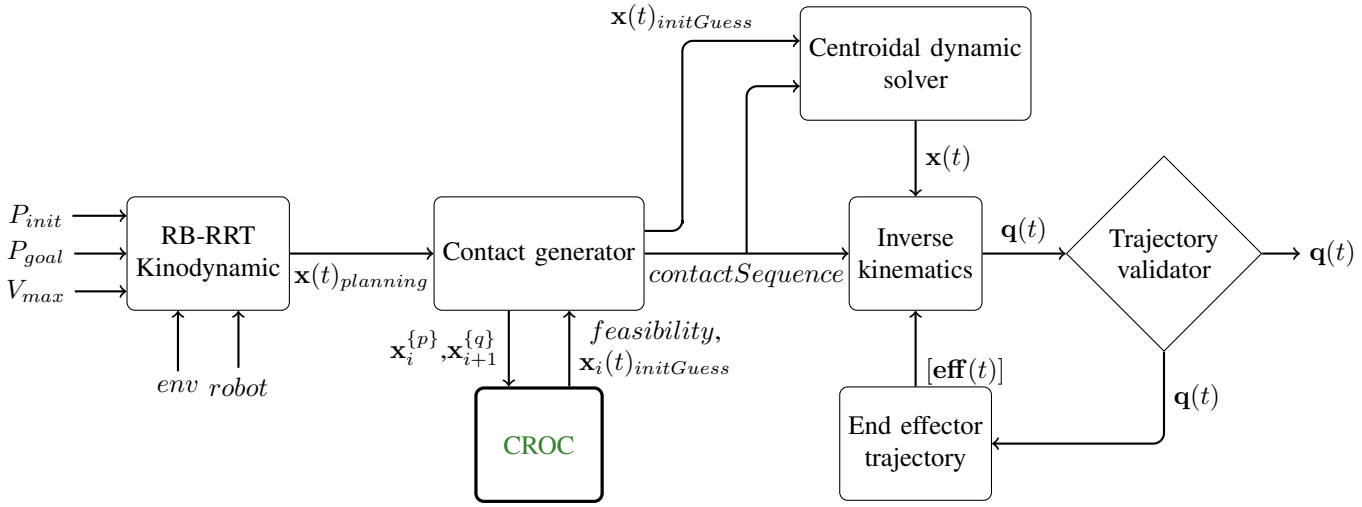

Fig. 10: Complete experimental framework.

A. RB-RRT kinodynamic planner

The first block generates a rough guide trajectory[5] for the root of the robot $\mathbf{x}(t)_{planning}$. It thus solves the sub-problem $\mathcal{P}_1$ defined in Figure 2. RB-RRT is a planning method based on the sampling-based RRT algorithm, which plans a guide trajectory for the geometric center of a simplified model of the robot. It thus solves a problem of lower dimension than planning in the configuration space of the real robot. The goal of this method is to find a trajectory for the root of the robot which will allow contact creation. This block was first presented in [15] and later extended to a kinodynamic version in [16], which is the one we use.

B. Contact generator with CROC as a feasibility criterion

The *contact generator* block computes a contact sequence, as a list of whole body postures along the discretized guide trajectory $\mathbf{x}(t)_{planning}$. This block solves the sub-problem $\mathcal{P}_2$ defined in Figure 2. It also generates an initial guess of the timing of each contact phase. This method was also introduced in [15].

CROC is used as a feasibility criterion by this contact generator. More precisely it is used as a filter to determine which transitions are unfeasible and discard them during the planning in order to produce contact sequence containing only feasible transitions. CROC will thus be called for each contact transitions considered by the contact generator ($\mathbf{x}_i^{\{p\}}$ and $\mathbf{x}_{i+1}^{\{q\}}$ in Figure 10) and output the feasibility of the given contact transition. The integration of CROC to this pipeline provides strong guarantees that the computed contact sequence will lead to a feasible CoM trajectory and thus that the centroïdal dynamics solver will converge with this contact sequence as input.

A byproduct of the feasibility test made with CROC is a feasible CoM trajectory between each adjacent contact phases ($\mathbf{x}(t)_{initGuess}$). This trajectory, not optimal, is used as an initial guess for a non-linear solver which will use it to compute an optimal trajectory.

[5]This guide is followed exactly to solve $\mathcal{P}_2$, but ignored at $\mathcal{P}_3$.

C. Centroidal dynamics solver

The *centroidal dynamics solver* block was proposed in [18], it takes as input the contact sequence found by the previous block, along with an initial guess of the timing of each phases and an initial guess of the CoM trajectory. The output of this block is a CoM trajectory that respects the centroïdal dynamics of the robot $\mathbf{x}(t)$ and minimizes a tailored cost function. This method solves an optimal control problem with a multiple-shooting algorithm implemented in MUSCOD-II [39].

The main interest of using a non-linear solver with the input of CROC is that the trajectory can then be refined globally (while the authors advise to use CROC with at most 3 contact phases), at the cost of a higher computational burden. CROC and the non linear solver are thus complementary: CROC does not provide an optimum, but is computationally efficient, which allows it to be used with a trial-and-error approach (ie. trying to solve problems that we dont know if a solution exist, until we find a solvable problem). Conversely, the non-linear solver is too computationally expensive to be used with a trial-and-error approach, but will in general propose a trajectory with a better optimum with respect to the optimized cost function. The proposed framework is designed to call this non-linear solver only once, with a problem that is known to have a solution.

The three different trajectories found in the framework of Figure 10 are shown in Figure 8, $\mathbf{x}(t)_{planning}$ is represented in black, $\mathbf{x}(t)_{initGuess}$ in yellow and orange and $\mathbf{x}(t)$ in green and blue. This figure shows a trajectory computed with CROC and the same trajectory refined with a non-linear solver as an illustration of the typical differences of both approaches.

D. Inverse kinematics

The whole-body motion $\mathbf{q}(t)$ is generated with a second order Inverse Kinematics solver, similar to [40]. This method

takes as input a reference trajectory for the CoM, as well as references for the trajectories of the end-effectors.

E. End-effector trajectory

In order to automatically generate valid end-effector trajectories for complex and constrained scenarios, we use a dedicated block. The trajectories computed are such that the whole limb is collision free and respect the kinematic constraints. The trajectories are represented as Bezier curves constrained to have a null initial and final velocity, acceleration and jerk and which respect velocity, acceleration and jerk bounds along the whole trajectory. In order to guarantee that the whole surface of the effector creates or breaks the contact at the same instant the curves are also constrained to have a velocity orthogonal to the contact surface for a small time step at the beginning and the end of the trajectory.

The positions of the control points of this Bezier curve are computed as the solution of a QP optimization method, using a cost function that defines a compromise between a reference optimal trajectory and a collision free one, provided by a probabilistic planner. This planner computes a geometric path for the moving limb that respects all the kinematic and collision constraints. However it may present discontinuities in velocity and higher derivatives and does not respect the dynamic constraints described in the previous paragraph. Moreover, as with any sampling-based method this path will not be optimal. Because of this, this geometric path will not be used directly as the end-effector trajectory but will be used inside the cost function of our optimization method.

Then several iterations are made between this optimization method and the inverse kinematics method, producing trajectories for the end-effectors and checking if the resulting whole-body motion is valid. If not, the weight of the cost associated to the solution of the geometric planner is increased at each iteration, until a valid motion is found.

VI. Experimental results

A. Experimental scenario

The complete experimental framework presented in the previous section was tested on several locomotion scenarios in semi structured environments, each scenario showing specific features or difficulties. We insist that the only manual inputs given to our framework were an initial and a goal position for the root of the robot. Most of the obtained motions are demonstrated in the companion video. They were validated either in a dynamics simulator or on the real robot.

1) Inclined platform crossing: This scenario requires the robot to go from one flat platform to the other by taking a step on an inclined platform (Figure 12). The scenario is designed such that no quasi-static solution exists to the problem, and is truly multi-contact for two reasons: firstly part of the motion occurs entirely on non-flat ground; secondly the problem is unfeasible if the right foot is the one selected to go first on the platform. CROC then allows to invalidate unfeasible contact sequences that would involve directly taking a step on the final platform, or take a step with the right foot first (Figure 13). It rather allows to find a solution where the left foot is used to step on the inclined platform (Figure 12). A feasible whole-body motion is demonstrated in the companion video.

Additionally, CROC also ensures that the left foot is positioned in such a way that the problem becomes feasible, which is not trivial considering the size of the solution space for the chosen step position (Figure 19(a)).

2) 10 cm high steps: This experimental setup is an industrial set of stairs shown in Figure 11 and 18(a). It consists of six 10 cm high and 30 cm long steps. This experiment was done with the HRP-2 robot. All the valid contact sequences produced contain at least 13 contact phases as the robot is kinematically constrained to put both feet on each step.

The complete motion is shown in the companion video. The crouching walk seen is required to avoid singularities in the knee of the extending leg, which are not tolerated by the low-level controller.

An example of unfeasible contact sequence filtered out by our feasibility criterion is depicted on Figure 14. All three configurations in this sequence are valid (ie. respect kinematics and dynamics constraints) but there isn't any valid centroidal trajectory between the last two configurations. Our feasibility criterion will filter out this kind of contact transitions during contact planning.

3) 15 cm high steps with handrail: This other set of stairs is composed of four 15 cm high steps and equipped with a handrail. The contact sequence is shown in Figure 18(b) and snapshots of the motion are shown in Figure 15. This is a typical multi-contact problem, showing an acyclic contact sequence with non co-planar contact surfaces. The problem was already solved in a previous work [17], but the input contact sequence and effector trajectories had to be manually selected from a large number of trials. In this paper, the only input is a root goal position at the top of the stairs.

A example of centroidal trajectory found by CROC for one contact transition in this scenario is shown in Figure 19(b).

4) Flat surface with ground level obstacles: This experimental setup consists of a flat floor with obstacles, shown in Figure 18(c) and (d). In (c) there is only one obstacle in front of the robot's initial position, in (d) we add smaller obstacles on the floor. This scenario shows that our planner is able to compute a valid guide root trajectory that avoids bigger obstacles and that our contact planner is able to avoid collision with smaller obstacles on the ground.

The difficulty of this scenario lies on the generation of collision free feet trajectories. Indeed, some obstacles are small enough to permit the feet to pass over the obstacles, but others are too high and require a lateral motion of the feet to avoid them. As shown in Figure 16 our method presented briefly in section V-E is able to find such trajectories automatically.

5) Uneven platforms: This setup consists of 30 cm long and 20 cm wide platforms, oriented of 15°around either the x or y axis. This scenario is particularly difficult for the contact planner because of all the possible collisions generated by the feet. We recall that the feet of HRP-2 are 24 cm long for 14 cm wide, which means that the platforms of this setup are only a few centimeters bigger than the feet of the robot. Because of this, there is really few collision free candidates positions for the feet. The probability of finding a contact position which

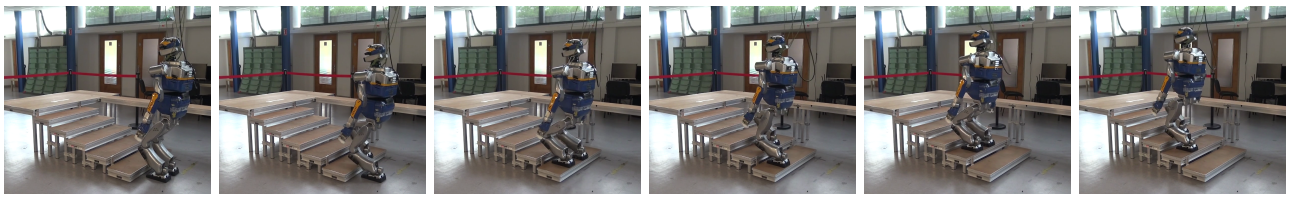

Fig. 11: Snapshots of the motion for the 10cm stairs, the complete motion is shown in the companion video.

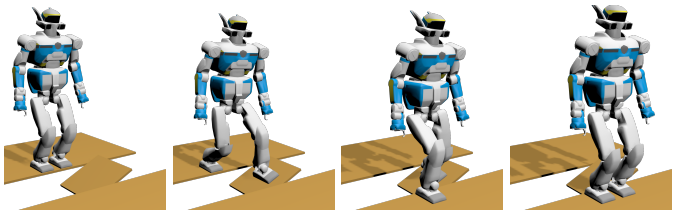

Fig. 12: Platform crossing scenario: no quasi-static solution exists for the flying phase where the left foot is on the inclined platform.

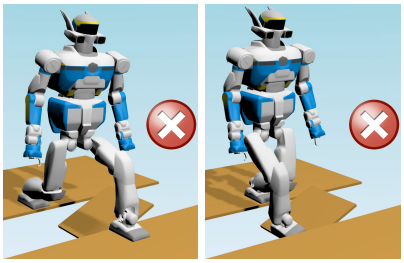

Fig. 13: Unfeasible stepping strategies invalidated by CROC.

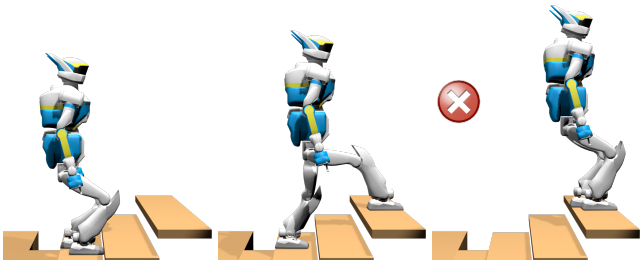

Fig. 14: Exemple of unfeasible contact transition detected by CROC and rejected during contact planning

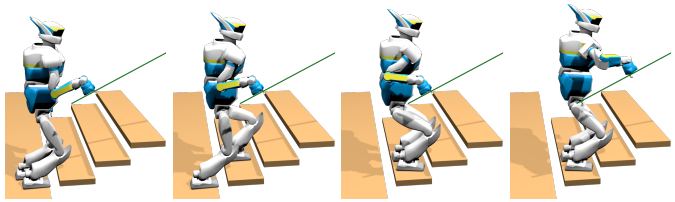

Fig. 15: A feasible multi-contact sequence for a stair climbing with handrail support on the HRP-2 robot automatically computed with our contact planner and CROC.

leads to a collision-free configuration while maintaining the equilibrium is extremely small for this setup.

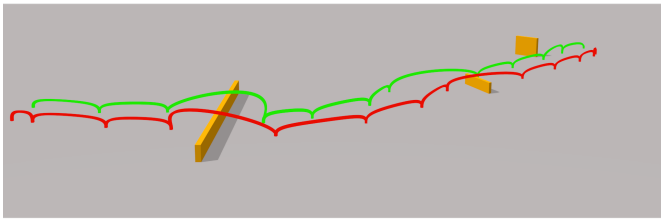

Fig. 16: Feet trajectories computed for scenario with ground level obstacles. Green for right foot and red for left foot.

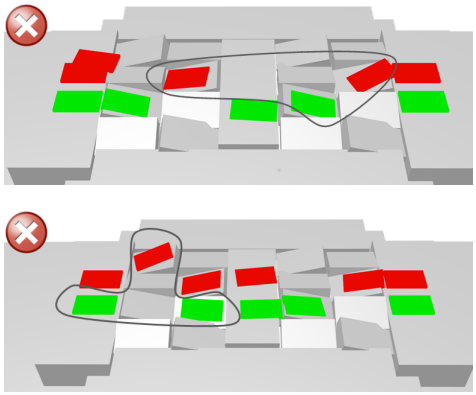

Fig. 17: Examples of unfeasible contact sequences filtered out by CROC. There doesn't exist any valid centroidal trajectory for the contact transitions encircled in black.

The contact sequence found is shown in Figure 18(e), snapshots of the motion are shown in Figure 1 and a motion for this scenario is shown in the companion video. These motions have been validated on the real robot.

The Figure 17 shows two examples of unfeasible contact sequence filtered out by CROC in this scenario.

6) Quadrupedal between inclined planes: The quadrupedal robot HyQ navigates between two planes inclined at $45°$. Figure 19(c) shows the the centroidal trajectory found by CROC in this scenario for one contact transition. This scenario shows that our method may be adapted to any type of legged robot.

B. Benchmarks

1) Using CROC as a feasibility criterion: In order to quantify the improvement of our contact planner from the use

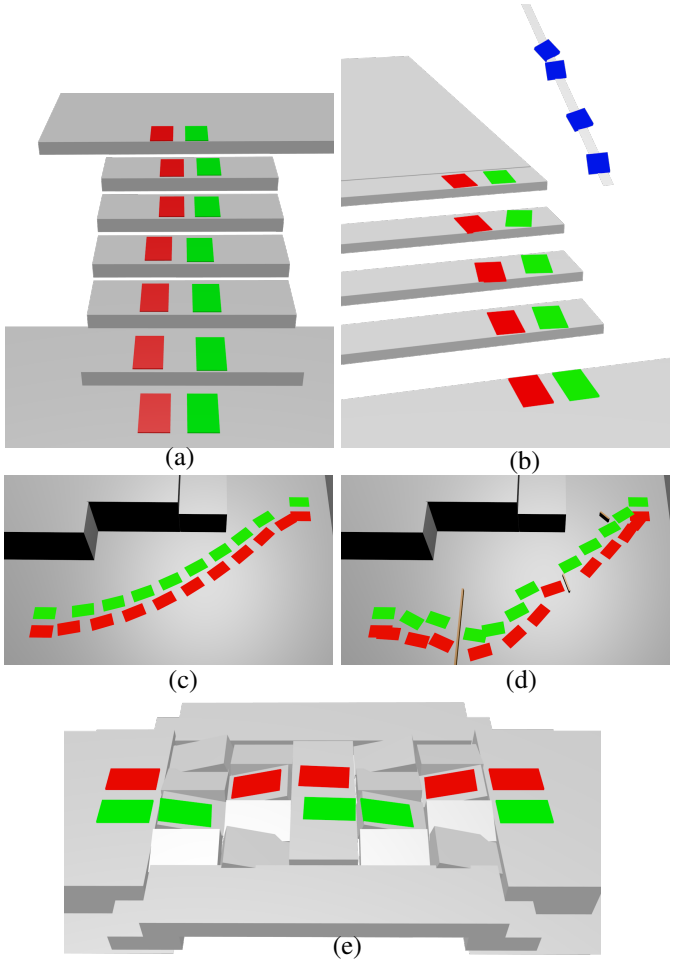

Fig. 18: Examples of contact sequences found with our framework. The color patches represent the planned contact location: green for right foot, red for left foot, blue for right hand.

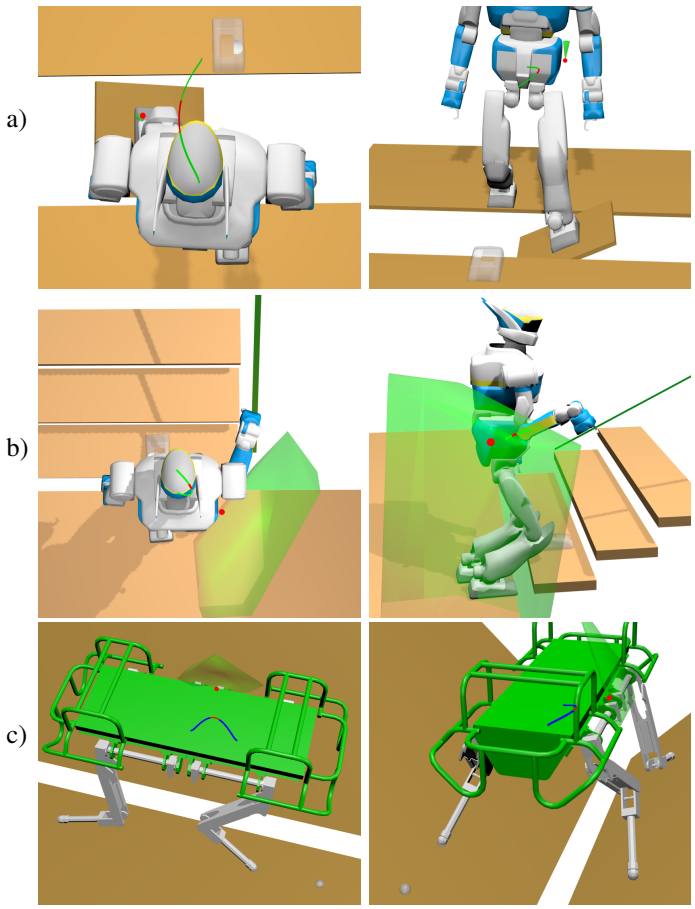

Fig. 19: Examples of centroidal trajectories found by our method. Green polytopes : valid position of $\mathbf{y}$ that verifies the constraints of the problem (24), red sphere : solution found for $\mathbf{y}$ for a given cost function (minimum of the squared acceleration norm). The red part of the trajectory is for the phase with $n_c - 1$ active contacts. The next contact is shown in transparency.

of CROC as a feasibility criterion, we used the following test procedure: for some of the scenarios presented in the previous section, we tried to solve the problem using our framework with and without using CROC as a feasibility criterion during the contact planning. We then measured the success rate of the centroidal dynamic solver with the contact plan found. The results are shown in Table V.

In the walking on flat floor scenario, CROC brings only a marginal improvement to our contact planner because our previously used heuristics were sufficient in this case to provide a feasible contact plan most of the time. However, in all the other cases the results empirically prove the main claim of this paper: using CROC as a feasibility criterion during the contact generation greatly increases the success rate of the centroidal trajectory generation because it produces contact plans with only feasible transitions. Another expected result is that there isn't any "false positive" found by our method: when CROC converges, the non linear solver always converges for the same transition.

The trade-off is an increase of the computation time required by the contact generator, from a few percents to nearly the double. This is explained partly by the addition of the time required to run CROC for each candidates, but mostly by the fact than we need to evaluate a lot more candidates before we find a valid one (ie. which lead to a feasible transition). This is shown in the column 4 of Table V, which provides the average number of contact candidates evaluated during the contact planning phase. Actually, depending on the scenario considered, only 7 to 16% of the total "contact planning" computation time is spent solving CROC problems. The rest of the time is mostly spent by projection methods and collision tests. This shows that our formulation is fast enough to be used inside a contact planner, without too much impact on its computation time.

2) Benchmarks of the complete framework: Table VI shows a benchmark of the performances of the complete motion planning framework presented in section V. We recall that this framework take as input only an initial and goal position for the center of the robot and produce as output a whole body motion.

We observe that the success rate is close to 100% except

Scenario	Method	Contact planning time (s)	Contact planning Evaluated candidates (avg.)	Centroidal dynamic solver success (%)
Walk (flat)	Without CROC	0.58	8.2	98
	With CROC	0.63	21.9	100
Stairs (3 steps)	Without CROC	0.61	24.4	52
	With CROC	0.87	92.9	100
Stairs (handrail)	Without CROC	1.26	147.2	31
	With CROC	1.87	384.0	100
Uneven platforms	Without CROC	3.91	679.1	15
	With CROC	7.59	3030	100

TABLE V: Evaluation of the feasibility of the contact plans found with or without CROC as a feasibility criterion. The *Contact Planning* column shows the computation time required by the contact planning phase and the average number of contact candidates evaluated during this phase. The last column shows the success rate of the centroidal trajectory generation method with the contact sequence found by the planner. Each scenario have been run 100 times.

Scenario	Motion duration (s)	Total time (s)	Success (%)
Walk (3 steps)	7.7	4.43	100
Walk with obstacles	55.02	51.5	99.3
Stairs	16.23	12.56	90.5
Stairs with handrail	23.13	18.09	88.05
Uneven platforms	14.94	17.83	83.5

TABLE VI: Performance analysis of the complete motion planning framework presented in section V, without the time required to compute collision free end-effector trajectory. *Motion duration* is the average duration of the solution, *total time* is the average computation time required to compute the motion. *Success* is the success rate of the complete framework.

for complex scenarios where it is still above 80% in the worst case. The main cause of failure in our current implementation of the framework is the inverse kinematics that may produce whole-body motions that do not respect the kinematic constraints or that are in self-collision. Concerning the computation time, in most of the cases we achieve interactive performances (ie. the computation time is smaller than the motion duration). In the worst case the computation time is greater than the motion duration, but only by a small margin.

As shown in Figure 20, the inverse kinematics method is currently the bottleneck of our framework and takes more than 60% of the total computation time.

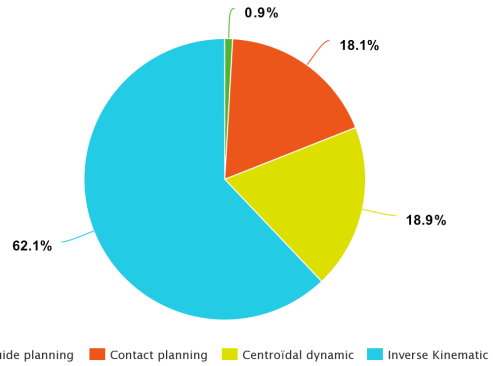

Fig. 20: Division of the computation time among the different methods of the motion planning framework.

VII. Conclusion

In this paper we introduce a continuous, accurate and efficient formulation of the centroidal dynamics of a legged robot, named *CROC*. Our method guarantees that it can compute valid centroidal trajectories that do not require discretization, nor use approximation or relaxation of the dynamic constraints. This formulation is convex yet conservative, but not limited to quasi-static motions. To our knowledge, this is the first method to combine all these properties.

Thanks to the computational efficiency of our method, requiring only a few milliseconds to solve the centroidal dynamic problem with three contact phases, we can use this method as a feasibility criterion during contact planning. The interest of this feasibility criterion has been demonstrated both qualitatively and empirically. Our results show that all the contact plans produced with CROC as a feasibility criterion lead to feasible centroidal dynamics problems. We also show that without using this feasibility criterion, the contact planner finds unfeasible contact sequences with a high probability on complex scenarios.

Moreover, the centroidal trajectory produced by CROC can be used to provide a relevant initial guess to a non linear solver, resulting in the improvement on the convergence rate and computation time of the non linear solver by comparison to the naive initial guess previously used.

Thanks to the continuous formulation proposed in this paper, we have the guarantee that the whole centroidal trajectory is valid, by opposition to the discretized methods of the state of the art that only guarantee that the discretized points of the trajectory are valid. We showed that the discretization may lead to a non negligible amount of invalid solutions where the trajectory is invalid between two valid discretization points, which emphasizes the interest of a continuous formulation. We believe that this continuous formulation of the constraints on the centroidal trajectory may be useful for all state-of-the-art methods, convex or non-linear. We leave the study of the feasibility and the interest of this application to a future work.

Finally, the feasibility criterion proposed in this paper permits us to complete our locomotion planning framework [41]. In this paper we showed that our framework is able to produce indifferently simple walking motions and multi-contact motions (ie. with non coplanar contacts and acyclic behaviors). These motions were validated in simulation or on the robot HRP-2. We also showed empirically that our framework presents a success rate close to 100% and present interactive computation times (the time required to compute a motion is smaller than the duration of this motion) in the studied scenarios, except for the most complex scenario where the computation time is approximately 20% greater than the duration of the motion, but still remain in the same order of magnitude. We believe that with an optimization of the implementation, interactive performances could be achieved even in the worst cases.

For future work we would like to try more complex motions

on the real robotic platform, but we are currently limited by the capabilities of our low level controller.

A. Handling whole-body approximations and uncertainties

The remaining source of approximation is shared with all centroidal-based methods, and comes from the whole-body constraints (joint limits, angular momentum and torques), which are only approximated or ignored in the current formulation. One solution could be to alternate centroidal optimization with whole-body optimization as other approaches do [19], however for the transition feasibility problem, this approach would result in an increased computational burden that is not compatible with the combinatorial aspect of the search. One way to improve the quality of this approximation is to integrate torque constraints [42], [43]. Expressing such constraints at the CoM level is considered for future work.

B. Application to 0 and 1 step capturability

The N-Step capturability problem consists in determining the ability of a robot (in a given state) to come to a stop (ie. null velocity and acceleration) without falling by taking at most N steps. It is used to detect and prevent fall.

We can easily change the constraints on $\mathbf{c}(t)$ defined in subsection III-A to remove the constraint on $\mathbf{c}_g$ and constrain $(\dot{\mathbf{c}}_g = \mathbf{0}, \ddot{\mathbf{c}}_g = \mathbf{0})$. With this set of constraints, the feasibility of FP (13) determines the 0-Step capturability. Similarly, FP (22) determines the 1-Step capturability.

For future work we would like to empirically determine the accuracy of our method with respect to this problem, using a framework similar to [14].

SOURCE CODE

Code available (C++/python) under a BSD-2 license: https://github.com/humanoid-path-planner/hpp-bezier-com-traj

ACKNOWLEDGMENT

Supports: ANR LOCO3D ANR-16-CE33-0003, ERC Actanthrope ERC-2013-ADG, H2020 Memmo ICT-780684.

REFERENCES

[1] S. Kajita, F. Kanehiro, K. Kaneko, K. Fujiwara, K. Harada, K. Yokoi, and H. Hirukawa, "Biped Walking Pattern Generation by using Preview Control of Zero-Moment Point," in *2003 IEEE International Conference on Robotics and Automation (ICRA)*, Taipei, Taiwan, Sep. 2003.

[2] J. Pratt, J. Carff, S. Drakunov, and A. Goswami, "Capture Point: A Step toward Humanoid Push Recovery," *2006 6th IEEE-RAS International Conference on Humanoid Robots*, 2006.

[3] I. Mordatch, E. Todorov, and Z. Popović, "Discovery of complex behaviors through contact-invariant optimization," *ACM Trans. on Graph.*, vol. 31, no. 4, pp. 43:1–43:8, 2012.

[4] R. Deits and R. Tedrake, "Footstep planning on uneven terrain with mixed-integer convex optimization," in *Humanoid Robots (Humanoids), 14th IEEE-RAS Int. Conf. on*, Madrid, Spain, 2014.

[5] M. Posa, C. Cantu, and R. Tedrake, "A direct method for trajectory optimization of rigid bodies through contact," *The Int. Journal of Robot. Research (IJRR)*, vol. 33, no. 1, pp. 69–81, Jan. 2014.

[6] A. W. Winkler, C. D. Bellicoso, M. Hutter, and J. Buchli, "Gait and Trajectory Optimization for Legged Systems through Phase-based End-Effector Parameterization," *IEEE Robotics and Automation Letters*, pp. 1–1, 2018. [Online]. Available: http://ieeexplore.ieee.org/document/8283570/

[7] T. Bretl, "Motion planning of multi-limbed robots subject to equilibrium constraints: The free-climbing robot problem," *The Int. Journal of Robot. Research (IJRR)*, vol. 25, no. 4, pp. 317–342, Apr. 2006. [Online]. Available: http://dx.doi.org/10.1177/0278364906063979

[8] K. Hauser, T. Bretl, and J.-C. Latombe, "Non-gaited humanoid locomotion planning," in *Humanoid Robots, 2005 5th IEEE-RAS Int. Conf. on*, 2005, pp. 7–12.

[9] A. Escande, A. Kheddar, and S. Miossec, "Planning contact points for humanoid robots," *Robotics and Autonomous Systems*, vol. 61, no. 5, pp. 428 – 442, 2013. [Online]. Available: http://www.sciencedirect.com/science/article/pii/S0921889013000213

[10] M. X. Grey, A. D. Ames, and C. K. Liu, "Footstep and motion planning in semi-unstructured environments using randomized possibility graphs," in *2017 IEEE International Conference on Robotics and Automation (ICRA)*, May 2017, pp. 4747–4753.

[11] P. Kaiser, C. Mandery, A. Boltres, and T. Asfour, "Affordance-based multi-contact whole-body pose sequence planning for humanoid robots in unknown environments," in *IEEE International Conference on Robotics and Automation*, 2018.

[12] T. Koolen, T. de Boer, J. R. Rebula, A. Goswami, and J. E. Pratt, "Capturability-based analysis and control of legged locomotion, part 1: Theory and application to three simple gait models," *I. J. Robotics Res.*, vol. 31, no. 9, pp. 1094–1113, 2012. [Online]. Available: https://doi.org/10.1177/0278364912452673

[13] J. E. Pratt, T. Koolen, T. de Boer, J. R. Rebula, S. Cotton, J. Carff, M. Johnson, and P. D. Neuhaus, "Capturability-based analysis and control of legged locomotion, part 2: Application to m2v2, a lower-body humanoid," *I. J. Robotics Res.*, vol. 31, no. 10, pp. 1117–1133, 2012. [Online]. Available: https://doi.org/10.1177/0278364912452762

[14] A. Del Prete, S. Tonneau, and N. Mansard, "Zero Step Capturability for Legged Robots in Multi Contact," *Accepted on IEEE Trans on Robotics*, 2018. [Online]. Available: https://hal.archives-ouvertes.fr/hal-01574687

[15] S. Tonneau, A. D. Prete, J. Pettré, C. Park, D. Manocha, and N. Mansard, "An efficient acyclic contact planner for multiped robots," *IEEE Transactions on Robotics*, vol. 34, no. 3, pp. 586–601, June 2018.

[16] P. Fernbach, S. Tonneau, A. D. Prete, and M. Taïx, "A kinodynamic steering-method for legged multi-contact locomotion," in *IEEE/RSJ International Conference on Intelligent Robots and Systems (IROS)*, Sept 2017, pp. 3701–3707.

[17] J. Carpentier, R. Budhiraja, and N. Mansard, "Learning Feasibility Constraints for Multi-contact Locomotion of Legged Robots," in *Robotics: Science and Systems*, Cambridge, MA, United States, Jul. 2017. [Online]. Available: https://hal.laas.fr/hal-01526200

[18] J. Carpentier and N. Mansard, "Multi-contact locomotion of legged robots," *Rapport LAAS n 17172. https://hal.laas.fr/hal-01520248. Conditionally accepted for IEEE Trans. on Robotics*, 2017.

[19] A. Herzog, N. Rotella, S. Schaal, and L. Righetti, "Trajectory generation for multi-contact momentum-control," in *Humanoid Robots (Humanoids), 15h IEEE-RAS Int. Conf. on*, Nov. 2015.

[20] H. Dai, A. Valenzuela, and R. Tedrake, "Whole-body motion planning with centroidal dynamics and full kinematics," in *Humanoid Robots (Humanoids), 14th IEEE-RAS Int. Conf. on*, Madrid, Spain, 2014, pp. 295–302.

[21] S. Caron, A. Escande, L. Lanari, and B. Mallein, "Capturability-based analysis, optimization and control of 3d bipedal walking," jan 2018, submitted. [Online]. Available: https://hal.archives-ouvertes.fr/hal-01689331

[22] B. Ponton, A. Herzog, S. Schaal, and L. Righetti, "A convex model of humanoid momentum dynamics for multi-contact motion generation," in *Proceedings of the 2016 IEEE-RAS International Conference on Humanoid Robots*, 2016.

[23] G. Mesesan, J. Englsberger, C. Ott, and A. Albu-Schffer, "Convex properties of center-of-mass trajectories for locomotion based on divergent component of motion," *IEEE Robotics and Automation Letters*, vol. 3, no. 4, pp. 3449–3456, Oct 2018.

[24] S. Lengagne, J. Vaillant, E. Yoshida, and A. Kheddar, "Generation of whole-body optimal dynamic multi-contact motions," *The International Journal of Robotics Research*, vol. 32, no. 9-10, pp. 1104–1119, 2013.

[25] P. Fernbach, S. Tonneau, and M. Taïx, "Croc: Convex resolution of centroidal dynamics trajectories to provide a feasibility criterion for the multi contact planning problem," in *IEEE/RSJ International Conference on Intelligent Robots and Systems (IROS)*, 2018.

[26] K. Fukuda and A. Prodon, *Double description method revisited*. Berlin, Heidelberg: Springer Berlin Heidelberg, 1996, pp. 91–111.

[27] D. E. Orin, A. Goswami, and S.-H. Lee, "Centroidal dynamics of a humanoid robot," *Autonomous Robots*, vol. 35, no. 2, pp. 161–176, Oct 2013.

[28] Z. Qiu, A. Escande, A. Micaelli, and T. Robert, "Human motions analysis and simulation based on a general criterion of stability," in *Int. Symposium on Digital Human Modeling*, 2011.

[29] S. Caron, Q.-C. Pham, and Y. Nakamura, "Leveraging Cone Double Description for Multi-contact Stability of Humanoids with Applications to Statics and Dynamics," in *Robotics, Science and Systems (RSS)*, 2015.

[30] A. Del Prete, S. Tonneau, and N. Mansard, "Fast Algorithms to Test Robust Static Equilibrium for Legged Robots," in *2016 IEEE International Conference on Robotics and Automation (ICRA)*, Stockholm, Sweden, 2016.

[31] S. Tonneau, A. D. Prete, J. Pettré, and N. Mansard, "2PAC: Two Point Attractors for Center of Mass Trajectories in Multi Contact Scenarios," Sep. 2017, accepted with major revisions for Trans. on Graphics. [Online]. Available: https://hal.archives-ouvertes.fr/hal-01609055

[32] J. M. (https://math.stackexchange.com/users/305862/jean marie), "Is the cross product of two bezier curves a bezier curve?" Mathematics Stack Exchange, uRL:https://math.stackexchange.com/q/2228976 (version: 2017-12-10). [Online]. Available: https://math.stackexchange.com/q/2228976

[33] F. Farshidian, M. Neunert, A. W. Winkler, G. Rey, and J. Buchli, "An efficient optimal planning and control framework for quadrupedal locomotion," in *Robotics and Automation (ICRA), 2017 IEEE International Conference on*. IEEE, 2017, pp. 93–100.

[34] R. Budhiraja, J. Carpentier, and N. Mansard, "Dynamics consensus between centroidal and whole-body models for locomotion of legged robots," in *ICRA 2019-IEEE International Conference on Robotics and Automation*, 2019.

[35] F. Gao, W. Wu, Y. Lin, and S. Shen, "Online safe trajectory generation for quadrotors using fast marching method and bernstein basis polynomial," in *2018 IEEE International Conference on Robotics and Automation (ICRA)*, May 2018, pp. 344–351.

[36] W. Sun, G. Tang, and K. Hauser, "Fast UAV trajectory optimization using bilevel optimization with analytical gradients," *CoRR*, vol. abs/1811.10753, 2018. [Online]. Available: http://arxiv.org/abs/1811.10753

[37] A. Makhorin, "Glpk (gnu linear programming kit)," *http://www. gnu. org/s/glpk/glpk. html*, 2008.

[38] J. Mirabel, S. Tonneau, P. Fernbach, A. K. Seppälä, M. Campana, N. Mansard, and F. Lamiraux, "Hpp: A new software for constrained motion planning," in *2016 IEEE/RSJ International Conference on Intelligent Robots and Systems (IROS)*, Oct 2016, pp. 383–389.

[39] D. B. Leineweber, I. Bauer, H. G. Bock, and J. P. Schlöder, "An efficient multiple shooting based reduced sqp strategy for large-scale dynamic process optimization. part 1: theoretical aspects," *Computers and Chemical Engineering*, vol. 27, no. 2, pp. 157 – 166, 2003. [Online]. Available: http://www.sciencedirect.com/science/article/pii/S0098135402001588

[40] L. Saab, O. E. Ramos, F. Keith, N. Mansard, P. Soures, and J. Y. Fourquet, "Dynamic whole-body motion generation under rigid contacts and other unilateral constraints," *IEEE Transactions on Robotics*, vol. 29, no. 2, pp. 346–362, April 2013.

[41] J. Carpentier, A. Del Prete, S. Tonneau, T. Flayols, F. Forget, A. Mifsud, K. Giraud, D. Atchuthan, P. Fernbach, R. Budhiraja, M. Geisert, J. Solà, O. Stasse, and N. Mansard, "Multi-contact Locomotion of Legged Robots in Complex Environments – The Loco3D project," in *RSS Workshop on Challenges in Dynamic Legged Locomotion*, Boston, United States, Jul. 2017, p. 3p. [Online]. Available: https://hal.laas.fr/hal-01543060

[42] R. Orsolino, M. Focchi, C. Mastalli, H. Dai, D. G. Caldwell, and C. Semini, "Application of wrench based feasibility analysis to the online trajectory optimization of legged robots," *IEEE Robotics and Automation Letters*, pp. 1–1, 2018.

[43] V. Samy, S. Caron, K. Bouyarmane, and A. Kheddar, "Post-impact adaptive compliance for humanoid falls using predictive control of a reduced model," in *2017 IEEE-RAS 17th International Conference on Humanoid Robotics (Humanoids)*, Nov 2017, pp. 655–660.